

EXPLICIT FORCE CONTROL V.S. IMPEDANCE CONTROL FOR MICROMANIPULATION

Bilal Komati *

Automatic Control and Micro-
Mechatronic Systems Department
FEMTO-ST Institute
25000 Besançon, France
Email: bilal.komati@femto-st.fr

**Muhammed R. Pac
Isura Ranatunga**

Next Generation Systems Group
Department of Electrical Engineering
University of Texas at Arlington
Texas 76010
Email: muhammed.pac@mavs.uta.edu

Cédric Clévy

Automatic Control and Micro-
Mechatronic Systems Department
FEMTO-ST Institute
25000 Besançon, France
Email: cclevy@femto-st.fr

Dan O. Popa

Next Generation Systems Group
Department of Electrical Engineering
University of Texas at Arlington
Texas 76010
Email: popa@uta.edu

Philippe Lutz

Automatic Control and Micro-
Mechatronic Systems Department
FEMTO-ST Institute
25000 Besançon, France
Email: philippe.lutz@femto-st.fr

ABSTRACT

This paper presents a study of different force control schemes for controlling contact during manipulation tasks at the microscale. Explicit force control and impedance control are compared in a contact transition scenario consisting of a compliant microforce sensor mounted on a microrobotic positioner, and a compliant microstructure fabricated using Silicon MEMS. A traditional double mass-spring-damper model of the overall robot is employed to develop the closed-loop force controllers. Specific differences between the two control schemes due to the microscale nature of contact are highlighted in this paper from the experimental results obtained. The limitations and tradeoffs of the two control laws at the microscale due to the presence of backlash are discussed. A simple method to deal with the pull-off force effects specific to the microscale is proposed. Future improvements of the impedance control schemes to include adaptation are discussed in order to handle objects with unknown stiffness.

1 INTRODUCTION

The development of microsystems (MEMS and MOEMS) has led to increasingly complex microstructures and smaller components. This development has increased the need of microassembly and micromanipulation. In the last few decades, researches have defined many micromanipulation and microassembly techniques [1], and have developed many robotic systems for microassembly [2,3]. The role of these robotic systems is to perform precise positioning and faster processes.

For automating microassembly or micromanipulation tasks, many of the past work deals with vision-based control [4, 5]. In many cases, vision feedback can only enable position control and ignores the interaction forces like gripping forces and contact forces between the grasped micropart and the substrate. In some other simple cases, force information can be derived from vision information if the contact conditions are simple and the environmental stiffness is known [6, 7]. However, this becomes difficult if both the gripper and the environment are compliant, and if the stiffness of the microparts is unknown. As a result, new microgrippers with integrated force sensing have been recently developed to enable force-feedback control during manipulation at the microscale, such as FemtoTools microgrippers [8].

* Address all correspondence to this author.

Furthermore, at the microscale, interaction forces experience significant nonlinear effects that cannot be simply modeled with a spring, such as adhesive forces. It is notably manifested by pull-off force which can be 84 times the $100\mu\text{m} \times 1000\mu\text{m} \times 1000\mu\text{m}$ silicon micropart weight [9]. Another important reason to take the microscale forces into consideration is the fragility of the components at small scale. Indeed, microparts and micro-grippers can easily break during manipulation and handling.

Issues relevant to robot force control at the macroscale are well known due to extensive research conducted in the 80's and 90's. Several classic control schemes have been developed including explicit force control, admittance control [10], impedance control [11, 12], and hybrid force/position control [13]. Recently, several of these control strategies have been used in microscale [14, 15] but no comparative study has been yet performed to see whether the physics of the microscale adds anything new to the existing body of knowledge.

This paper investigates differences between force control schemes due to scaling. The work in this paper is limited to studying explicit force and impedance controllers, due to the fact that many other schemes are based on them. For instance, admittance control is similar to the impedance control since the admittance is the inverse of the impedance and the hybrid force/position requires to have many axes and to control some axes in position and the others in force.

The importance of this work is that it provides a good theoretical and experimental base for research using force control for micromanipulation and microassembly applications. The paper is organized as follows. The experimental setup used in this paper and some of the microscale specific effects are explained in Section 2. The system modeling and some force control laws formulation are developed in Section 3. Section 4 presents the experimental results obtained for the force control laws integrated into the experimental setup. Section 5 concludes the article.

2 FORCE CONTROL AT MICROSACLE

A motivating microscale scenario for this paper is depicted in this section and some of the microscale specific effects are explained in order to take them into consideration for the control design.

2.1 Experimental Setup

The hardware shown in Fig. 1 and 2 was used to control the interaction between a MEMS force sensor and a compliant environment. A microstructure made of $100\mu\text{m}$ thick Silicon via microfabrication was used as the spring mechanism of the environment. A force sensing probe from FemtoTools AG, Switzerland, used as a manipulator, was attached to a motorized stage and the spring mechanism was attached to a stationary base. The stage was controlled through a National Instruments, Austin, Texas,

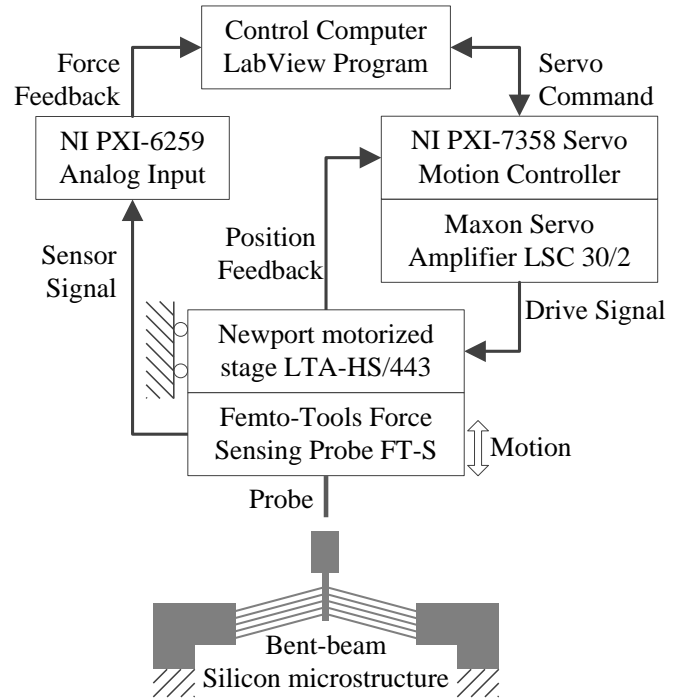


FIGURE 1. THE DIAGRAM OF THE EXPERIMENTAL SETUP.

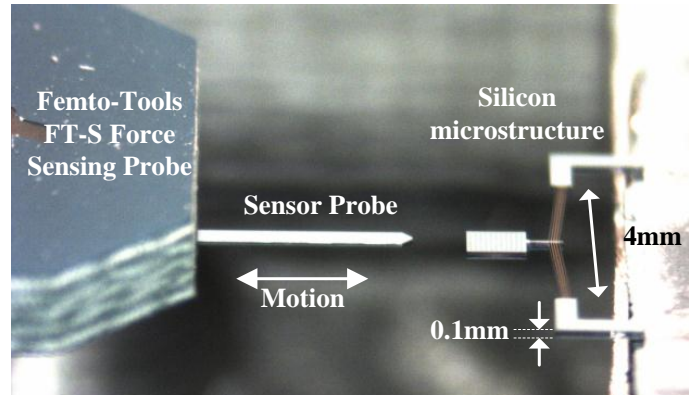


FIGURE 2. SIDE IMAGE OF THE SETUP USED.

USA servo motion controller. The force feedback was acquired through an analog input data acquisition board, and the controller was implemented in using NI LabVIEW.

The motorized stage from Newport Corporation, Santa Ana, California, USA, has a minimum incremental motion of $0.1\mu\text{m}$ and an uni-directional repeatability of $0.5\mu\text{m}$. The stage also has a backlash of $12\mu\text{m}$.

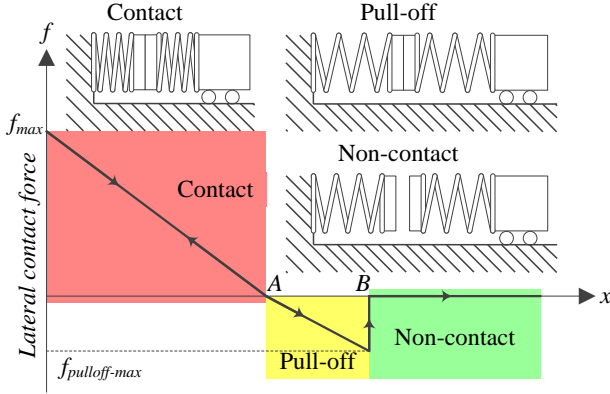


FIGURE 3. THE EVOLUTION OF THE LATERAL CONTACT FORCE IN THE PRESENCE OF PULL-OFF FORCE DURING LEFT SIDE AND RIGHT SIDE CONTACTS IN THE RAIL.

2.2 Scaling Issues

There are many differences between contact models at macroscale and microscale. We can mention the different predominant forces, the different signal to noise ratios for sensors and the added nonlinearities/positioning errors for actuators. Surface force being predominant at the microscale, it is required to evaluate the influence of surface forces during the studied task. These forces appear when a contact between the environment and the force sensor happens. To automatically achieve a contact/non-contact transition at the microscale, pull-off force has to be accounted for. It is the force necessary to break a contact due to stiction and has a predominant role when contact happens between microscale objects.

It was shown in [9] that the pull-off force can reach $196\mu\text{N}$ for a planar $50\mu\text{m} \times 50\mu\text{m}$ silicon contact surface that can typically happen in the present case. During the contact/non contact transition, the breaking of the lateral contact may induce a pull-off force for each side of the contact. In this case, the evolution of the lateral contact force according to the position of the micropart can follow curves in Fig. 3, i.e once a contact (micropart/environment) happens, the pull-off force acts as a sticking effect. As shown in Fig. 3, an opposite force is applied during the withdrawal to break the contact. At point A, the lateral contact force is zero but the contact remains due to adhesive force. The contact is broken at B when enough force is applied to balance the adhesive force.

The signal to noise ratio is another difference between the microscale and macroscale. This is caused by the fact that the signals at the microscale have large bandwidths, small amplitudes and high noise. The noise is due to the type of components used, their sensitivity to the environmental conditions (temperature, humidity, small vibrations) and the microfabrication uncertainties. To deal with these microscale specificities, some filters

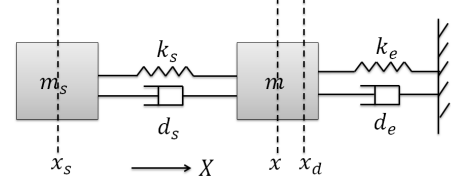


FIGURE 4. SYSTEM MODEL BASED ON SPRING DAMPER

should be integrated taking into consideration not to change the dynamics of the signals. The bandwidth of microsystems usually contains high frequencies, so using low pass filters will affect the dynamics of the system. In addition, the controller must be able to deal with the noise and must not confuse between contact force and noise.

3 SYSTEM MODELING AND CONTROL

In this section, the model of the system used in this paper is discussed. Then, explicit force control and impedance control are studied showing the differences between these two strategies.

3.1 Model of the system

The contact interaction between a robot and the environment is typically modeled by mass-spring-damper models. In this paper, the proposed models are divided into two parts: an environment part modeled by a mass-spring-damper and a gripper part modeled also by mass-spring-damper. This corresponds to a flexible-gripper, flexible-part interaction scenario typically encountered at the microscale. The proposed model is shown in Fig. 4.

In Fig. 4, m is the mass of the contact surface (gripper + environment), m_s , k_s and d_s are respectively the mass, the stiffness and the damping of the gripper, k_e and d_e are respectively the stiffness and the damping of the environment, x_s is the actual position of the stage which moves the gripper, x_d and x are respectively the desired and the actual position of the environment. x , x_s and x_d are relative positions to the initial positions before contact.

During contact, the dynamics equation is given by (1):

$$m\ddot{x} = F_{gripper \rightarrow m} + F_{environment \rightarrow m} \quad (1)$$

Where $F_{gripper \rightarrow m}$ and $F_{environment \rightarrow m}$ are respectively the forces exerted from the spring and damper of the gripper to the mass and from the spring and damper of the environment to the mass. The dynamics of the system is given by (2):

$$m\ddot{x} + f_m + f_e = 0 \quad (2)$$

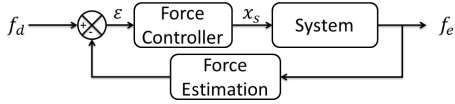


FIGURE 5. EXPLICIT FORCE CONTROL SCHEME

where f_m is the force exerted by the mass on the gripper and f_e is the force exerted on the environment. f_m given by (3), is the force measured by the force sensor.

$$f_m = -F_{gripper \rightarrow m} = d_s(\dot{x} - \dot{x}_s) + k_s(x - x_s) \quad (3)$$

The force exerted on the environment f_e is given by (4).

$$f_e = -F_{environment \rightarrow m} = k_e x + d_e \dot{x} \quad (4)$$

Robots are usually controlled by motor efforts (force or torque). In some applications, and especially at the microscale, the robots are controlled in position or velocity instead. In this case, we change the existing control schemes where the calculated command is the force to a controller in which the calculated command by the controller is an incremental position or velocity of a moving stage. The aim is to control the force exerted to the environment f_e in order to guarantee the stability of the grasp in micromanipulation, and also to not break components.

3.2 Explicit Force Control

The explicit force control aims to control the force exerted on the environment f_e in reference to a desired force f_d [16]. Two types of explicit force control exist: force-based and inner position loop based. The most commonly discussed technique in the literature is the force-based explicit force control in which P, PI or PD controllers are used [17–19]. In this article, the inner position loop based explicit force control is used because the robotic system is controlled by position. The explicit force control scheme used in this paper is given by Fig. 5. The force controller calculates the position command x_s using the error ϵ between the desired force and the measured force exerted on the environment f_e and sends it to the controlled stage. If f_e is not measured, it should be estimated using the position and another measurement, if possible, f_m . The form of the controller changes in function of the application and of the requirements of the system. The most commonly used controllers are a P, PI or PD controllers. These controllers are used for their simplicity and their effectiveness. Other types of controllers could be used as well. An incremental controller like the one used in [14] could also be used (see Fig. 6). The idea of this controller is to compare the desired force to the output force and then the controller sends

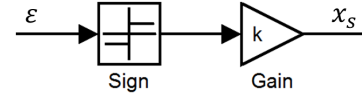


FIGURE 6. INCREMENTAL CONTROLLER

a relative position command to go forward or backward with a predefined step (gain) in function of the sign of the difference ($\epsilon = f_d - f_e$). The advantage of this type of controller is that it is easy to implement, robust and effective even if the system is nonlinear. The drawbacks of this controller is that the response of the system is slow or it chatters as a function of the gain of the controller (see Section 4). A PD controller could be used if the reference force is constant which is usually the case. In this case, the command could be calculated using (5).

$$x_s = K_p(f_d - f_e) - K_d \dot{f}_e \quad (5)$$

Where f_e in (5) is the measured or the estimated force exerted on the environment.

3.3 Impedance Control

The aim of the impedance control is to control the dynamics of contact. The dynamics of contact are set to follow a desired impedance. It has been demonstrated in [20] that an impedance controller with force feedback contains an explicit force controller. In the case of impedance control with force feedback, the force is also controlled in reference to a desired force. Using the Laplace transform of (2) and (3), (6) could be derived. The position x is replaced by $X(s) = \frac{f_m(s)}{d_s s + k_s} + X_s(s)$ using (3):

$$m s^2 X_s(s) + \frac{m s^2 + d_s s + k_s}{d_s s + k_s} F_m(s) + F_e(s) = 0 \quad (6)$$

where s is the complex argument, X_s , F_m and F_e are the Laplace transforms of x_s , f_m and f_e respectively.

The desired impedance proposed by Hogan in [11], using the Laplace transform, is given by (7).

$$X_d(s) - X(s) = \frac{1}{M_d s^2 + D_d s + K_d} F_e(s) \quad (7)$$

where X_d is the desired position, M_d , D_d and K_d define the desired impedance parameters of the system. Using (6) and (7), the command sent to the stage x_s is given by (8):

$$X_s(s) = \frac{M_d s^2 + D_d s + K_d}{(M_d - m) s^2 + D_d s + K_d} X_d(s) - \frac{(M_d - m) s^2 + (D_d - d_s) s + (K_d - k_s)}{(d_s s + k_s) ((M_d - m) s^2 + D_d s + K_d)} F_m(s) \quad (8)$$

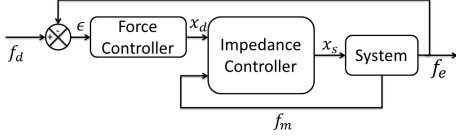


FIGURE 7. IMPEDANCE CONTROL SCHEME

An external force control loop could be added to the internal impedance controller. The goal of this controller is not only to control the impedance of the contact but also to control the exerted force in reference to a desired force. The final impedance control scheme used in this paper is given by Fig. 7 using the controller equation defined in (8) where the controller has two inputs, the desired position x_d , calculated by the force controller, and the force measured by the force sensor f_m . The output of the controller x_s is the position command sent to the system. The force controller in Fig. 7 could be a P, PD, or PI controller. The proportional force controller is chosen in this case because of its simplicity and to guarantee the stability of the controller which is not the case with the integral controller.

4 EXPERIMENTAL RESULTS

In this section, the different types of force control discussed in Section 3 are tested, the dynamical behaviors will be shown and the performances will be compared. These experiments were carried out on the experimental system depicted in Fig. 1 and 2 at the University of Texas at Arlington. The control schemes shown in Fig. 5 and 7 consist of motion control, force sensing hardware and a control program developed in LabView as in Fig. 1.

4.1 Estimation of the force exerted on the environment

Before detailing the experimental results, the force feedback is the force measured by the force sensor f_m which is not the same as the force exerted on the environment f_e as shown in (2). Thus, f_e should be estimated. Using (2), (3) and (4) f_e could be estimated using two possible equations (9) or (10). In the following two equations, the position x is replaced by $X(s) = \frac{F_e(s)}{d_e s + k_e}$ using (4):

$$F_e(s) = \frac{d_s d_e s^2 + (d_s k_e + d_e k_s) s + k_s k_e}{m s^2 + (d_s + d_e) s + (k_s + k_e)} X_s(s) \quad (9)$$

$$F_e(s) = \frac{d_e s + k_e}{m s^2 + d_e s + k_e} F_m(s) \quad (10)$$

In (9), f_e is estimated using the measurement of the position, x_s , the measurement of the stage position given by the encoder, and

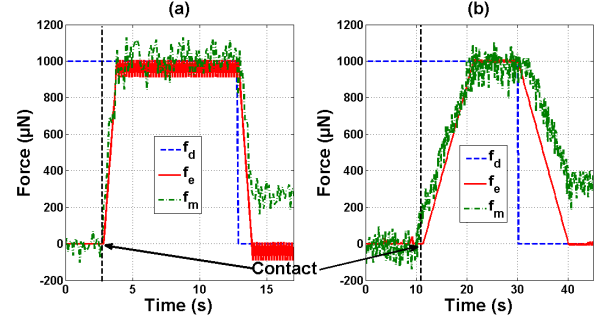


FIGURE 8. SYSTEM RESPONSE FOR AN INCREMENTAL FORCE CONTROLLER (a) WITH A BIG STEP OF THE CONTROLLER, (b) WITH A SMALL STEP OF THE CONTROLLER

assumed noiseless. Thus, (9) estimates f_e without noise. However, (10) estimates f_e using f_m and \dot{f}_m . Where f_m is the force measured by the force sensor which is noisy (for the force sensor used the noise has amplitude of $100 \mu\text{N}$). Since \dot{f}_m is very noisy, f_e will also be very noisy. The amplitude of noise could be reduced, in our case, using a low pass filter to filter the measured force f_m . Using the estimation of f_e given by (9) appears to be a good idea. However, a backlash problem of the stage causes a big problem for estimating f_e because the measurement of the stage will not be reliable if many reference signals are applied. Thus, (10) is used to estimate f_e .

Before starting the experiments, the parameters used for control m , d_s and d_e are calculated theoretically and k_e and k_s are estimated experimentally. The calculation of the mass was done using the volume of the system. The damping coefficients were calculated using the values of the damping of the Silicon and the sections of the system. k_s was estimated by applying a force by the force sensor to a stiff environment and measuring the displacement of the stage. k_e was estimated by applying a force by the force sensor to the flexible environment used and measuring the displacement of the environment. The values used for calculating the control laws are $m \approx 70 \text{ mg}$, $d_s \approx d_e \approx 0.3 \text{ Ns/m}$, $k_e \approx 20 \text{ N/m}$ and $k_s \approx 5000 \text{ N/m}$.

4.2 Experimental results for the explicit force control

As discussed in Section 3, two types of explicit force control are tested and compared: a PD controller and an incremental controller. The response of the system in presence of an incremental control and using the estimation of f_e given in (9) is shown in Fig. 8.

First, the effect of the step (gain in Fig. 6) of the incremental controller influences the behavior of the system. Big step increments imply a low response time but the amplitude of chattering in the static part is also big. However, small step increments implies a big response time and a smaller amplitude of chattering

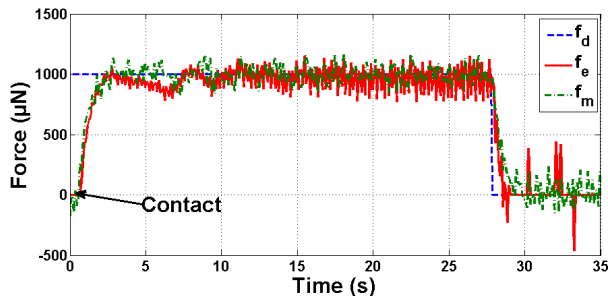


FIGURE 9. SYSTEM RESPONSE FOR A PD FORCE CONTROLLER

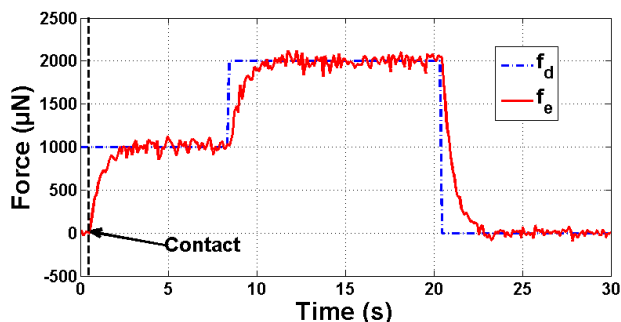


FIGURE 10. SYSTEM RESPONSE FOR AN IMPEDANCE CONTROLLER

in the static part. Secondly, in these figures, the effect of backlash appears. The estimated force f_e returns to zero while the measured force f_m does not. The force feedback being the estimated value of f_e using (9), the controller controls the estimated force f_e correctly but the estimation of f_e is wrong because of the backlash problem.

Using a PD controller could be a solution to have a good response time without chattering in the static part. This type of controller is used because it is simple and gives good performance. The controller used is given by (5). The performance is given in Fig. 9. In this case, the estimation of f_e given by (10) with a low pass filter is used. Fig. 9 shows that f_e and f_m follow the same shape and they are almost the same in the static part. However, f_e and f_m are noisy. The response time of the system is good (≈ 1 s). It could be improved by modifying the gains of the PD controller but there is a risk that the system will become unstable in this case.

4.3 Experimental results for the impedance control

The impedance control block shown in Fig. 7 and the controller given in (8) are used to control the system. Fig. 10 shows

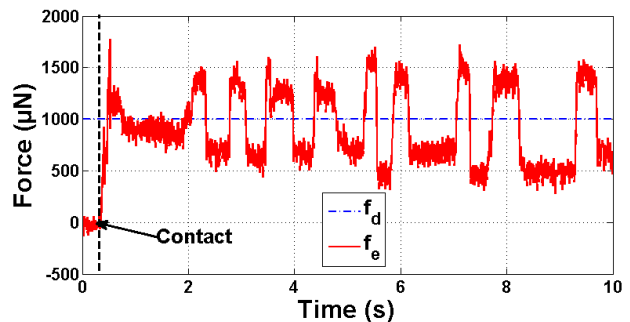


FIGURE 11. SYSTEM RESPONSE TO IMPEDANCE CONTROL IN PRESENCE OF A STIFF ENVIRONMENT

the response of the system using the impedance control scheme defined. The system response is a first order with a response time of ≈ 1 s. The behavior is close to the explicit force control. This fact is because the impedance control is used with an external force control feedback. The main difference is in terms of the impedance of the system during contact. The impedance control aims to set the dynamics of the system to a desired impedance defined by the user. Comparing f_e in Fig. 9 and Fig. 10, the response of the controlled system is first order in Fig. 10 while in Fig. 9 it exhibits a transient behavior before setting f_e to f_d .

In impedance control, the desired dynamics of the response of the system is set using three parameters M_d , D_d and K_d . Thus, the controller controls at the same time the impedance of the control and the f_e in reference to f_d . Some experiments have shown that the use of the proposed impedance control scheme is limited to a flexible environment. However, the stability of the proposed controller is not guaranteed for a very stiff environment as shown in Fig. 11.

A simple comparison between the explicit force control and impedance control results shown in Fig. 9 and Fig. 10 shows that the explicit force controller is simpler than the impedance controller in terms of controller complexity. Both of them are robust. The contact transition for the impedance control is better than the explicit force control. The impedance control is more flexible in design (3 parameters to control) and shows good disturbance rejection.

For instance, the controller is able to set f_e to zero when a zero force reference is applied but it is not able to break the contact due to pull-off force. The specific effect due to the microscale is discussed in the following section.

4.4 Experimental results showing the pull-off force effect

As shown in Section 2, the pull-off force could appear when a contact happens. The pull-off force acts as a sticking effect. During the experiment, once the contact happens and we aim to

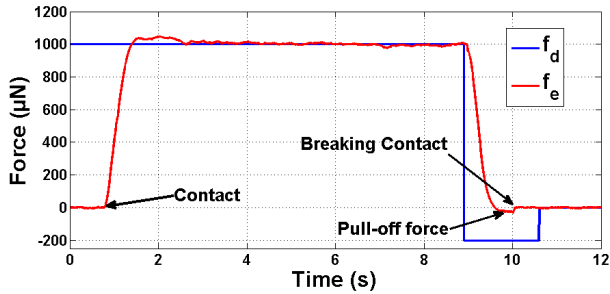


FIGURE 12. THE PULL-OFF FORCE APPEARS WHILE BREAKING THE CONTACT. EXPERIMENT DONE FOR IMPEDANCE CONTROL SCHEME

separate the contact, setting the desired force to zero will not separate the contact, the contact will persist although the measured force is zero. An easy way to separate the contact is to apply a negative force reference for a short time and then return the desired force to zero. When a negative force reference is applied, the controller aims to set the desired force to the reference and then a command is sent to the stage to come back and then the contact is broken. During this phase, a negative measured force appears due to the pull-off force. This force is not constant during the experiments. It varies as a function of many variables (angle, surface, etc...) [9]. Fig. 12, shows the effect of pull-off force on the system. The pull-off force is the negative part of the force f_e . It appears while breaking the contact. The contact is not broken directly when the force returns to zero.

Fig. 12 shows also the effect of modifying the estimated values of the parameters. This modification changes the response of the system to a second order with an overshoot in place of a first order response. Other experiments have shown that the impedance controller behavior is acceptable until a parameter change of 40%. More than 40%, the response of the system will not be acceptable and the system could become unstable.

The problem of signal to noise ratio is avoided, in our case, by adding a low pass filter to the signal because the bandwidth of the system does not contain high frequencies. The results show that the noise level of the output signal f_e is small due to filtering.

5 CONCLUSION

In this paper, a comparison between explicit force control and impedance control for microscale manipulation applications was carried out using experimental results. It was shown that unique effects specific to the microscale affect the effectiveness of these force controllers. Not surprisingly, impedance control showed better performance than explicit force control. Similar to the macroscale, impedance control is better at controlling the

dynamics of contact between the manipulator and object. But unlike the macroscale, impedance control is also better at exerting forces on the environment, and more robust at handling flexible components with unknown stiffness. The impedance control scheme used is robust for flexible components and for a small variation of elements. The use of impedance control is limited in presence of a stiff environment. Another limitation would be the parameter uncertainties. Results have shown that the impedance control scheme used in this paper was able to deal with up to 40% change in the parameters. It was shown that most of the challenges in force control are common for microscale and macroscale but the main differences are the presence of pull-off force at microscale and the signal to noise ratio. A simple method to deal with the pull-off force was proposed. Filtering solves the main problems of the signal to noise ratio, at the expense of bandwidth. To use the impedance control, the parameters of the system should be known m, k_e, k_s, \dots which was the case in this paper. If some parameters are unknown, an adaptive impedance controller could be used to estimate the unknown parameters during the experiments. This will be the focus of future work.

This paper shows that the use of impedance control for microscale is a promising topic in coming years specially with the progress of force control for some microassembly and micromanipulation applications. The impedance control could be used for many microassembly tasks (for picking and releasing a micropart, for guiding a micropart in a rail or for inserting a micropart in a hole). This work was done for a 1 DOF moving stage and it will be extended to more complex systems.

ACKNOWLEDGMENT

The authors would like to thank the Net4m project for funding the travel of Bilal Komati from the University of Franche-Comté to the University of Texas at Arlington, the region Franche-Comté in France and the University of Texas at Arlington Research Institute for funding the equipment and hosting the experiments presented in this paper.

REFERENCES

- [1] Savia, M., and Koivo, H. N., Aug. 2009. "Contact micromanipulation-survey of strategies". *IEEE/ASME Transactions on Mechatronics*, vol. 14, no. 4, pp. 504–514.
- [2] Dechev, N., Ren, L., Liu, W., Cleghorn, W., and Mills, J., May 2006. "Development of a 6 degree of freedom robotic micromanipulation for use in 3d mems microassembly". *IEEE International Conference on Robotics and Automation, Orlando, FL*, p. 281288.
- [3] Das, A. N., Zhang, P., Lee, W. H., Stephanou, H., and Popa, D., 2007. " μ^3 : Multiscale, deterministic micro-nano assembly system for construction of on-wafer microrobots".

- IEEE International Conference on Robotics and Automation, Roma, Italia*, pp. 461 – 466.
- [4] Wang, L., Ren, L., Mills, J., and Cleghorn, W., 2010. “Automated 3-d micrograsping tasks performed by vision-based control”. *IEEE Transactions on Automation Science and Engineering*, **7**, pp. 417 – 426.
- [5] Anis, Y., Holl, M., and Meldrum, D., 2010. “Automated selection and placement of single cells using vision-based feedback control”. *IEEE Transactions on Automation Science and Engineering*, **7**, July, pp. 598 – 606.
- [6] Greminger, M., and Nelson, B., March 2004. “Vision-based force measurement”. *IEEE Transactions on Pattern Analysis and Machine Intelligence*, pp. 290 – 298.
- [7] Liu, X., Sun, Y., Wang, W., and Lansdorp, B. M., July 2007. “Vision-based cellular force measurement using an elastic microfabricated device”. *Journal of Micromechanics and Microengineering*, **17**.
- [8] <http://www.femtotools.com/index.php?id=products-g>.
- [9] Rabenoroso, K., Clevy, C., Lutz, P., Gauthier, M., and Rougeot, P., 2009. “Measurement of pull-off force for planar contact at the microscale”. *Micro Nano Letters*, **4**, pp. 148 – 154.
- [10] Seraji, H., 1994. “Adaptive admittance control: An approach to explicit force control in compliant motion”. In Jet Propulsion Laboratory California Institute of Technology Pasadena, CA 91109.
- [11] Hogan, N., 1985. “Impedance control - an approach to manipulation. i - theory. ii - implementation. iii - applications”. *ASME Transactions Journal of Dynamic Systems and Measurement Control B*, **107**, p. 1 – 24.
- [12] Singh, S., and Popa, D., Dec 1995. “An analysis of some fundamental problems in adaptive control of force and impedance behavior: theory and experiments”. *IEEE Transactions on Robotics and Automation*, **11**, pp. 912 – 921.
- [13] Raibert, M., and Craig, J. J., 1981. “Hybrid position/force control of manipulators”. *Transactions of ASME, Journal of Dynamic Systems, Measurement, and Control*, **102**, pp. 126–133.
- [14] Komati, B., Rabenoroso, K., Clévy, C., and Lutz, P., 2013. “Automated guiding task of a flexible micropart using a two-sensing-finger microgripper”. *IEEE Transactions on Automation, Science and Engineering*, **PP, Issue: 99**, pp. 1 – 10, paper online at <http://ieeexplore.ieee.org/>, DOI 10.1109/TASE.2013.2241761.
- [15] Lu, Z., Chen, P. C. Y., Ganapathy, A., Zhao, G., Nam, J., Yang, G., Burdet, E., Teo, C., Meng, Q., and Lin, W., 2006. “A force-feedback control system for micro-assembly”. *Journal of Micromechanics Microengineering*, **16**, pp. 1861–1868.
- [16] Volpe, R., and Khosla, P., Nov 1993. “A theoretical and experimental investigation of explicit force control strategies for manipulators”. *IEEE Transactions on Automatic Control*, **38**, *Issue: 11*, pp. 1634 – 1650.
- [17] An, C., and Hollerbach, J., Mar 1987. “Dynamic stability issues in force control of manipulators”. *IEEE International Conference on Robotics and Automation*, pp. 890 – 896.
- [18] Colgate, E., and Hogan, N., May 1989. “An analysis of contact instability in terms of passive physical equivalents”. *IEEE International Conference on Robotics and Automation*, pp. 404 – 409.
- [19] Eppinger, S., and Seering, W., Mar 1987. “Understanding bandwidth limitations in robot force control”. *IEEE International Conference on Robotics and Automation*, **4**, pp. 904 – 909.
- [20] Volpe, R., Sept. 1990. “Real and artificial forces in the control of manipulators: Theory and experiments”. PhD thesis, Carnegie Mellon Univ., Dep. of Physics, The Robotics Institute.